European Journal of Nuclear Medicine and Molecular Imaging (2019) 46:2339–2347
https://doi.org/10.1007/s00259-019-04441-1

ORIGINAL ARTICLE

Enlarged perivascular spaces and florbetapir uptake in patients with intracerebral hemorrhage

Nicolas Raposo[1,2] · Mélanie Planton[1,2] · Pierre Payoux[2,4] · Patrice Péran[2] · Jean François Albucher[1,2] · Lionel Calviere[1,2] · Alain Viguier[1,2] · Vanessa Rousseau[3] · Anne Hitzel[2,4] · François Chollet[1,2] · Jean Marc Olivot[1,2] · Fabrice Bonneville[2,5] · Jérémie Pariente[1,2]

Received: 3 May 2019 / Accepted: 16 July 2019 / Published online: 29 July 2019

Abstract

Purpose Enlarged perivascular spaces in the centrum semiovale (CSO-EPVS) have been linked to cerebral amyloid angiopathy (CAA). To get insight into the underlying mechanisms of this association, we investigated the relationship between amyloid-β deposition assessed by 18F-florbetapir PET and CSO-EPVS in patients with acute intracerebral hemorrhage (ICH).

Methods We prospectively enrolled 18 patients with lobar ICH (suggesting CAA) and 20 with deep ICH (suggesting hypertensive angiopathy), who underwent brain MRI and 18F-florbetapir PET. EPVS were assessed on MRI using a validated 4-point visual rating scale in the centrum semiovale and the basal ganglia (BG-EPVS). PET images were visually assessed, blind to clinical and MRI data. We evaluated the association between florbetapir PET positivity and high degree (score> 2) of CSO-EPVS and BG-EPVS.

Results High CSO-EPVS degree was more common in patients with lobar ICH than deep ICH (55.6% vs. 20.0%; $p = 0.02$). Eight (57.1%) patients with high CSO-EPVS degree had a positive florbetapir PET compared with 4 (16.7%) with low CSO-EPVS degree ($p = 0.01$). In contrast, prevalence of florbetapir PET positivity was similar between patients with high vs. low BG-EPVS. In multivariable analysis adjusted for age, hypertension, and MRI markers of CAA, florbetapir PET positivity (odds ratio (OR) 6.44, 95% confidence interval (CI) 1.32–38.93; $p = 0.03$) was independently associated with high CSO-EPVS degree.

Conclusions Among patients with spontaneous ICH, high degree of CSO-EPVS but not BG-EPVS is associated with amyloid PET positivity. The findings provide further evidence that CSO-EPVS are markers of vascular amyloid burden that may be useful in diagnosing CAA.

Keywords Intracerebral hemorrhage · Cerebral amyloid angiopathy · Perivascular spaces · Amyloid PET · Florbetapir

Introduction

Cerebral small vessel diseases (SVD), including mainly cerebral amyloid angiopathy (CAA) and hypertension angiopathy (HA) are the most important causes of spontaneous intracerebral hemorrhage (ICH) in the elderly [1]. HA affects predominantly small deep perforating vessels whereas CAA affects cortical and leptomeningeal vessels [2–4]. Understanding the underlying SVD has important clinical implications because CAA and HA are characterized by different risks of ICH recurrence [5, 6]. The presence and distribution of MRI hemorrhagic markers such as cerebral microbleeds (CMB) [7] or cortical superficial siderosis (cSS) [8] are suggestive of the underlying vasculopathy. Enlarged perivascular spaces (EPVS) are emerging markers of SVD that may result from enlargement of the potential space, possibly secondary to impaired interstitial fluid drainage [9, 10]. Recent imaging

This article is part of the Topical Collection on Neurology

✉ Nicolas Raposo
raposo.n@chu-toulouse.fr

1 Department of Neurology, Hôpital Pierre-Paul Riquet, Centre Hospitalier Universitaire de Toulouse, Place Baylac, 31059 Toulouse Cedex 9, France

2 Toulouse NeuroImaging Center, Université de Toulouse, Inserm, UPS, Toulouse, France

3 Department of Epidemiology, Centre Hospitalier Universitaire de Toulouse, Toulouse, France

4 Department of Nuclear Medicine, Hôpital Pierre-Paul Riquet, Centre Hospitalier Universitaire de Toulouse, Toulouse, France

5 Department of Neuroradiology, Hôpital Pierre-Paul Riquet, Centre Hospitalier Universitaire de Toulouse, Toulouse, France

studies have shown that EPVS in the centrum semiovale (CSO-EPVS) suggest underlying CAA whereas EPVS in the basal ganglia (BG-EPVS) indicate HA [11]. As failure of perivascular clearance of Aβ may be involved in the accumulation of Aβ in CAA [12] and cortical vessels are predominantly affected by CAA [2], CSO-EPVS observed in CAA may reflect the impairment of Aβ perivascular clearance.

To get insight into mechanisms linking CSO-EPVS and CAA, we explored in the current study the association between EPVS burden and topography and 18F-florbetapir, a positon emission tomography (PET) radiotracer shown to label vascular amyloid deposits in CAA [13, 14] in patients with acute spontaneous ICH. We tested the hypothesis that florbetapir PET positivity is associated with high CSO-EPVS degree, but not with high BG-EPVS degree. We also investigated the association between florbetapir PET positivity and EPVS predominance pattern in the CSO (CSO-EPVS > BG-EPVS burden) and BG (BG-EPVS > CSO-EPVS burden).

Materials and methods

Patient selection

Participants were recruited from the Toulouse Hospital (France) as part of a prospective single-center cohort study (ClinicalTrial.gov no. NCT01619709) [14]. The study was approved by Toulouse-Purpan Hospital Ethical Standards Committee on Human Experimentation. Written informed consent was obtained from each participant or a legally authorized representative.

We enrolled patients with acute symptomatic primary supratentorial ICH who underwent brain MRI and 18F-florbetapir PET. We excluded patients with (1) infratentorial ICH, (2) traumatic ICH, (3) secondary causes of ICH (such as vascular malformation, cerebral venous thrombosis, hemorrhagic infarction, or brain tumor), and (4) preexisting cognitive decline defined by a score of 3.4 or above on the long version of the Informant Questionnaire on Cognitive Decline in the Elderly (IQCODE) [15]. Based on ICH location, patients were categorized as having (1) lobar ICH (consistent with CAA) when ICH was restricted to cortical-subcortical regions or (2) deep ICH (consistent with HA) when ICH involved the thalamus or basal ganglia.

Data collection

Demographic and baseline clinical data were prospectively recorded and analyzed. Hypertension was defined as any use of antihypertensive medication or documented elevated blood pressure > 140/90 mmHg, before admission. APOE genotyping was performed in all participants.

MRI acquisition and analysis

MR images were acquired from all subjects using the same 3-T MRI scanner (Philips 3.0T Intera Achieva, Philips, Best, the Netherlands) according to a standardized protocol. They included 3D T1-weighted (in-plane resolution 1 × 1 mm, 170 contiguous slices) and 3D fluid attenuated inversion recovery (FLAIR) (in-plane resolution 1 × 1 mm, 160 contiguous slices) and T2*-weighted gradient recalled echo (T2*-GRE) sequences (reconstructed resolution 1 × 1 × 4 mm, repetition time = 1052 ms, echo time = 16 ms, flip angle = 18°, field of view = 230 × 182, 140 slices).

All images were reviewed by investigators blinded to the clinical and PET data according to the Standards for Reporting Vascular Changes on Neuroimaging (STRIVE) [9].

The presence, number, and distribution (lobar or deep) of CMB (diameter < 5 mm) were evaluated on the T2*-GRE images according to the current consensus criteria [7]. The presence and extent (focal [≤ 3 sulci] or disseminated [≥ 4 sulci]) of cSS were visually assessed according to recommended criteria [16]. Periventricular and deep white matter hyperintensities (WMH) were visually assessed on axial FLAIR images on the 7-point Fazekas rating scale [17]. EPVS were assessed by two trained raters (NR and FB) on axial T1-weighted images using a validated 4-point visual rating scale (0 = no EPVS, 1 = < 10 EPVS, 2 = 11–20 EPVS, 3 = 21–40 EPVS, and 4 = > 40 EPVS) [18, 19]. EPVS were defined as < 3-mm round or linear CSF isointense lesions (T2 hyperintense and T1/FLAIR hypointense with respect to brain) along the course of penetrating arteries. Lacunes were distinguished from EPVS by their larger size (>3 mm), spheroid shape, and surrounding hyperintensity on FLAIR. EPVS were rated in BG and CSO. The numbers refer to EPVS on one side of the brain: after reviewing all relevant slices for the anatomical area being assessed, the slice and side with the highest number of EPVS were recorded. In patients with large ICH that limited accurate rating, EPVS were evaluated in the contralateral hemisphere. For each region (BG and CSO), EPVS were categorized as high (score > 2) or low (score ≤ 2) degree. The interrater reliability for the class of EPVS was excellent for CSO-EPVS ($\kappa = 0.83$) and BG-EPVS ($\kappa = 0.82$). Additionally, patients were categorized based on EPVS predominance pattern in the CSO or BG, as previously described [11]: (1) CSO-EPVS predominance pattern (CSO-EPVS > BG-EPVS score); (2) BG-EPVS predominance pattern (BG-EPVS > CSO-EPVS score); and (3) non-predominance EPVS pattern (BG-EPVS = CSO-EPVS score).

Table 1 Baseline clinical and imaging characteristics of patients with lobar ICH and deep ICH

	Lobar ICH ($n = 18$)	Deep ICH ($n = 20$)	p value[a]
Age (years), mean ± SD	67.2 ± 12.1	64.4 ± 11.3	0.46
Female, *n* (%)	9 (50.0)	6 (30.0)	0.21
Hypertension, *n* (%)	5 (27.8)	18 (90.0)	< 0.0001
IQCODE, mean ± SD	3.04 ± 0.21	2.98 ± 0.53	0.85
APOE ε2 and/or ε4 allele, *n* (%)	10 (55.6)	2 (10.0)	0.003
High EPVS degree (grade > 2)			
High BG-EPVS degree, *n* (%)	1 (5.6)	5 (25.0)	0.18[b]
High CSO-EPVS degree, *n* (%)	10 (55.6)	4 (20.0)	0.02
CMB count, median (IQR)	4.5 (0–10.0)	5 (1–10.5)	0.65
Strictly lobar CMB, *n* (%)	12 (66.7)	2 (10.0)	< 0.001
Strictly deep CMB, *n* (%)	0 (0.0)	5 (25.0)	0.05[b]
Presence of cSS, *n* (%)	10 (55.6)	1 (5.0)	0.001
Severe (Fazekas 5–6) WMH, *n* (%)	9 (50.0)	8 (40.0)	0.54
Florbetapir PET positivity, *n* (%)	10 (55.5)	2 (10.0)	0.003
Florbetapir SUVr positive, *n* (%)	11 (61.1)	4 (20.0)	0.01

[a] Wilcoxon test for quantitative variables and chi^2 test for qualitative variables

[b] Fisher test

BG, basal ganglia; *CMB*, cerebral microbleeds; *CSO*, centrum semiovale; *cSS*, cortical superficial siderosis; *EPVS*, enlarged perivascular spaces; *ICH*, intracerebral hemorrhage; *IQCODE*, Informant Questionnaire on Cognitive Decline in the Elderly; *SUVr*, standard uptake value ratio; *WMH*, white matter hyperintensities

Florbetapir PET imaging acquisition and analysis

Florbetapir PET scans were performed on a Biograph™ 6 TruePoint™ (Siemens Medical Solutions, Munich, Germany) high-resolution hybrid PET/CT scanner (3D detection mode, producing images with 1 × 1 × 1.5-mm voxels and a spatial resolution of 5 mm full width at half maximum at the field of view center) using procedures that we previously described [14]. A 10-min acquisition started 50 min after intravenous injection of 3.7 MBq/kg weight of 18F-florbetapir. PET data were corrected for partial volume effects using the point spread function (PSF) model implemented by Siemens (HD-PET©).

The 18F-florbetapir PET images were visually assessed, by two board-certified nuclear medicine physicians (AH and PiP), blinded to all clinical and diagnostic information, who were experienced in amyloid scan assessment. They were trained to do binary classification of scans as either florbetapir positive if there was some significant florbetapir cortical retention (two or more brain areas in which there was reduced or absent gray/white matter contrast or one or more areas in which gray matter radioactivity was intense) or as florbetapir negative if there was no significant florbetapir cortical retention (clear gray/white matter contrast) as previously described [20]. To ensure that the raters were blind from ICH location, a mask of the ipsilesional hemisphere was used for the visual assessment of florbetapir PET. The interrater reliability for the visual assessment of the 18F-florbetapir PET scans was excellent ($\kappa = 1$). Figure 1 shows examples of EPVS distribution in Lobar ICH and deep ICH cases with corresponding florbetapir PET.

In addition to the visual rating of PET images, we performed a semiautomated quantitative analysis of cortical florbetapir retention that we previously described [14]. Mean regional cortical florbetapir standard uptake value ratios (SUVr) were computed in each participant using five cortical gray matter ROIs (frontal, insular, temporal, parietal, occipital). We used the whole cerebellum as reference for SUVr calculation. Global cortical florbetapir SUVr was calculated as the average of the SUVr value in each ROIs in the hemisphere not affected by ICH. Based on SUVr analysis, a florbetapir PET was defined as positive (SUVr positive) when the global cortical florbetapir SUVr was greater than 1.8, a threshold value derived from a single-center florbetapir PET study on patients with primary ICH to define positive CAA cases [14].

Statistical analyses

Baseline clinical and imaging characteristics of patients with lobar ICH and deep ICH were compared using the χ^2 test or Fisher's exact test for qualitative variables and the Wilcoxon rank-sum test for quantitative variables, as appropriate.

We performed appropriate univariate tests to compare clinical data, MRI characteristics, and florbetapir PET (visual) positivity data between patients with high (score > 2) and

those with low (score ≤ 2) degree of CSO-EPVS and BG-EPVS.

Logistic regression models were used to identify factors associated with high CSO-EPVS degree. Clinical characteristics, MRI markers of SVD, and florbetapir PET positivity were tested in univariable models. For the multivariable analysis, candidate covariates included all variables with $p < 0.1$ in univariable analysis and other potential confounders. Clinical and imaging variables were age, history of hypertension, strictly lobar CMB (presence), cSS (presence), severe WMH (Fazekas' score 5 or 6), and florbetapir PET positivity. Final model was obtained using backward elimination strategy and contained only factors significant at 5%.

Additionally, we explored the association between EPVS predominance pattern (CSO-EPVS predominance; BG-EPVS predominance; non-predominance EPVS pattern) and florbetapir PET positivity using χ^2 test or Fisher's exact test, as appropriate.

As a sensitive analysis, we explored the associations of florbetapir PET positivity based on the SUVr analysis (SUVr positive) with (1) high vs. low EPVS degree in the CSO and BG and (2) EPVS predominance pattern.

Statistical testing was conducted at an alpha level of 0.05 (two-tailed). Data were analyzed with SAS® software, version 9.4 (SAS Institute).

Results

Study participants

A total of 38 patients (mean age 65.7 ± 11.6 years; female 39.5%) with acute primary ICH were prospectively included between January 2012 and March 2016: 18 with lobar ICH (13 with probable CAA, 2 with definite CAA, and 3 with possible CAA, based on the modified Boston criteria [8]) and 20 with deep ICH. The participants had no pre-ICH cognitive impairment (IQCODE ≤ 3.4).

Clinical and imaging characteristics of patients are summarized in Table 1. Overall, 14 (36.8%) patients had high CSO-EPVS degree, 6 (15.8%) had high BG-EPVS degree, and 3 (7.9%) had high degree of both CSO-EPVS and BG-EPVS. High CSO-EPVS degree was more commonly observed in patients with lobar ICH than deep ICH (55.6% vs. 20.0%; $p = 0.02$). In contrast, high BG-EPVS degree was rarely observed in patients with lobar ICH (5.6%) and tended to be more frequent in patients with deep ICH (25.0%; $p = 0.18$). Florbetapir PET was visually assessed as positive in 10 (55.5%) patients with lobar ICH compared with 2 (10.0%) patients with deep ICH ($p = 0.003$). Among patients with lobar ICH, florbetapir PET was visually positive in all patients with definite CAA, 7 (53.8%) with probable CAA, and 1

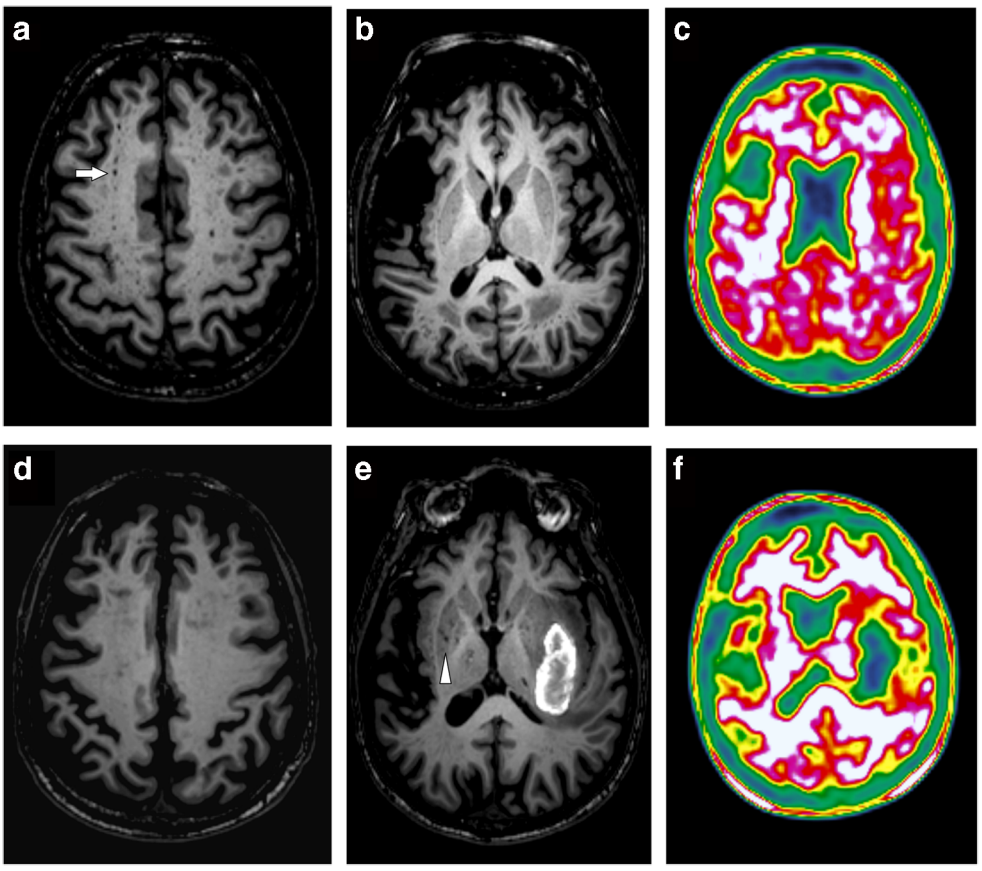

Fig. 1 Examples of enlarged perivascular space patterns with corresponding florbetapir PET in lobar and deep intracerebral hemorrhage. a–c Patient with lobar ICH. Axial T1-weighted MRI shows high degree of enlarged perivascular spaces in the centrum semiovale (a; white arrow) and a low degree in the basal ganglia (b). The corresponding 18F-florbetapir PET (c) was positive. d–f Patient with deep ICH. Axial T1-weighted MRI shows low degree of enlarged perivascular spaces in the centrum semiovale (d) and a high degree in the basal ganglia (e; white head arrow). The corresponding 18F-florbetapir PET (f) was negative

Table 2 Comparison of clinical and MRI characteristics between patients with high (grade > 2) vs. low (grade ≤ 2) EPVS degree in the centrum semiovale and the basal ganglia

	High CSO-EPVS degree	Low CSO-EPVS degree	*p* value[b]	High BG-EPVS degree	Low BG-EPVS degree	*p* value[b]
No.	14	24	–	6	32	–
Clinical characteristics						
Age, mean ± SD	70.2 ± 9.2	63.1 ± 12.2	0.07	66.5 ± 10.1	65.6 ± 12.0	0.86
Female, No. (%)	6 (42.9)	9 (37.5)	0.74	1 (16.7)	14 (43.8)	0.37[c]
Hypertension, No. (%)	5 (35.7)	18 (75.0)	0.02	5 (83.3)	18 (56.3)	0.37[c]
Diabetes, No. (%)	2 (14.3)	5 (20.8)	0.99[c]	2 (33.3)	5 (15.6)	0.30[c]
APOE ε2 and/or ε4 allele, No. (%)	6 (42.9)	6 (25.0)	0.30[c]	1 (16.7)	11 (34.4)	0.64[c]
MRI markers of SVD						
Lobar CMB count, median (IQR)	6 (0–21)	1.5 (0–3.5)	0.14	4 (1–12)	2 (0–6.5)	0.41
Deep CMB count, median (IQR)	0 (0–0)	1 (0–4)	0.08[c]	4.5 (0–5)	0 (0–1)	0.08
cSS presence, No. (%)	6 (42.9)	5 (20.8)	0.27[c]	0 (0.0)	11 (34.4)	0.15[c]
Severe WMH[a], No. (%)	10 (71.4)	7 (29.2)	0.01	4 (66.7)	13 (40.6)	0.38[c]

[a] Fazekas' score 5 or 6

[b] Wilcoxon test for quantitative variables and chi^2 test for qualitative variables

[c] Fisher test

BG, basal ganglia; *CMB*, cerebral microbleeds; *CSO*, centrum semiovale; *cSS*, cortical superficial siderosis; *EPVS*, enlarged perivascular spaces; *WMH*, white matter hyperintensities

(33.3%) with possible CAA. Based on the SUVr analysis, florbetapir PET was classified as positive in 11 (61.1%) patients with lobar ICH compared with 4 (20%) with deep ICH ($p = 0.01$).

High vs. low EPVS degree in the CSO and BG

Comparison of characteristics between patients with high and low EPVS degree in the CSO and BG is shown in Table 2. Compared with those with low CSO-EPVS degree, patients with high CSO-EPVS degree were more likely to have severe WMH and less likely to have hypertension. Among patients with high CSO-EPVS degree, 8 (57.1%) were visually rated as florbetapir PET positive compared with 4 (16.7%) with low CSO-EPVS degree ($p = 0.01$; Fig. 2a). The proportion of patients with florbetapir PET positive was similar between subjects with high BG-EPVS degree and low BG-EPVS degree (33.3% vs. 31.3%; $p = 0.92$). In the SUVr analysis, 8 (57.1%) patients with high CSO-EPVS degree were classified as positive, compared with 7 (29.2%) with low CSO-EPVS degree ($p = 0.09$). Florbetapir SUVr positivity was similar between patients with high BG-EPVS degree and low BG-EPVS degree (33.3% vs. 40.6%; $p = 0.737$).

In multivariable logistic regression analysis, florbetapir PET positivity (odds ratio (OR) 6.44, 95% confidence interval (CI) 1.32–38.93; $p = 0.03$) and severe WMH presence (OR 5.87, 95% CI 1.28–33.48; $p = 0.03$) were independently associated with the presence of high CSO-EPVS degree (Table 3).

EPVS predominance pattern

Among the whole cohort, 14 (36.8%) patients had a CSO-EPVS predominance pattern (CSO > BG), 7 (18.4) had a BG-EPVS predominance pattern (BG > CSO), and 17 (44.7) had a non-predominant EPVS pattern (BG = CSO). A CSO-EPVS predominance pattern was more commonly observed in patients with lobar ICH than deep ICH (61.1% vs. 15.0%; $p = 0.003$). Among patients with deep ICH, a BG-EPVS predominance pattern was detected in 5 (25%) subjects compared with 2 (11.1%) patients with lobar ICH ($p = 0.41$).

Among patients with a CSO-EPVS predominance pattern, 8 (57.1%) had a visually positive florbetapir PET, compared with 4 (23.5%) with a non-predominant EPVS pattern and none with a BG-EPVS predominance pattern ($p = 0.02$; Fig. 2b). A florbetapir SUVr positivity was observed in 7 (50.0%) patients with a CSO-EPVS predominance pattern, 6 (35.3%) with a non-predominant EPVS pattern, and 2 (28.6%) with a BG-EPVS predominance pattern ($p = 0.57$).

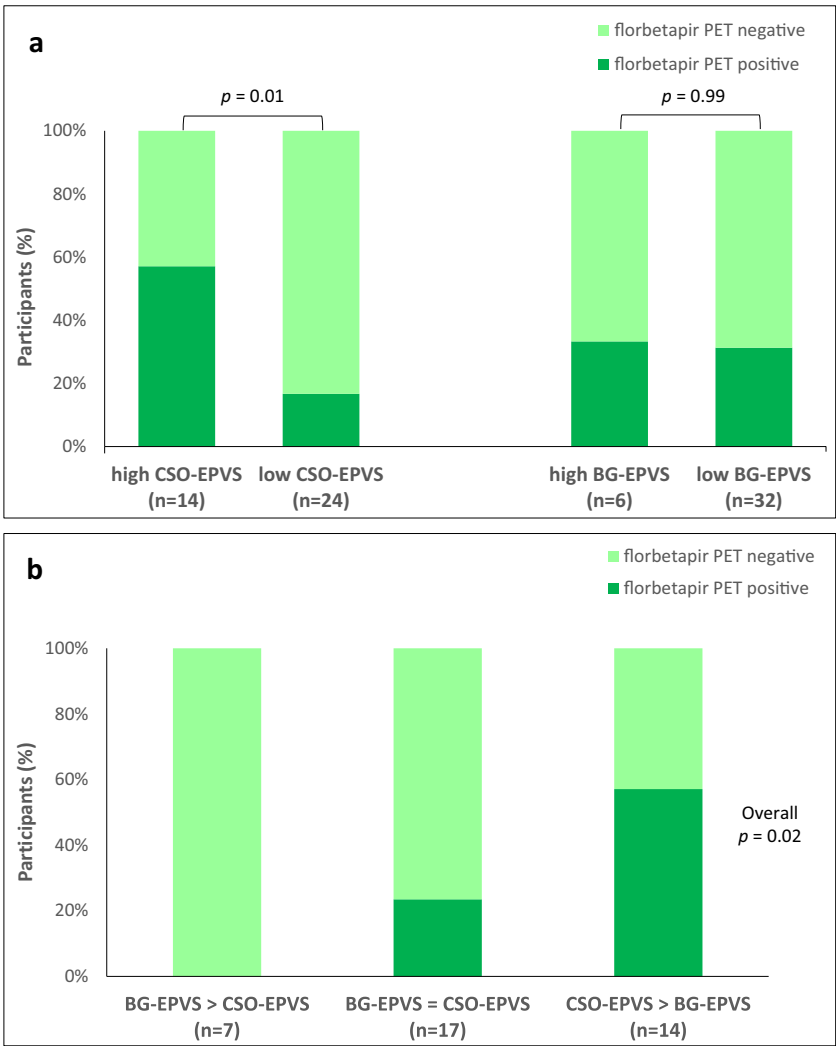

Fig. 2 Florbetapir PET visual analysis according to the distribution of enlarged perivascular spaces. (a) Comparison of florbetapir PET between patients with high (grade > 2) and low (grade ≤ 2) enlarged perivascular spaces degree in the centrum semi ovale and the basal ganglia. (b) Florbetapir PET according to the enlarged perivascular spaces predominance pattern. Abbreviations: BG, = basal ganglia; CSO, = centrum semi-ovale; EPVS, = enlarged perivascular spaces

Discussion

In this prospective single-center study of patients with acute spontaneous ICH, high CSO-EPVS degree was more common in patients with lobar ICH than in deep ICH and was associated with florbetapir PET positivity. By contrast, high BG-EPVS were rarely observed in patients with lobar ICH and were not associated with florbetapir PET positivity. Additionally, florbetapir PET positivity was considerably more common in patients with a CSO-EPVS predominance pattern than in those with BG-EPVS predominance pattern. These findings provide further evidence that in patients with symptomatic ICH, CSO-EPVS could be markers of vascular amyloid burden that may be useful in detecting underlying CAA.

EPVS are emerging neuroimaging markers of SVD. Previous studies suggest that BG-EPVS are associated with hypertension and imaging markers of HA such as WMH and lacunes [18, 21]. Conversely, CSO-EPVS appear to be associated with both AD and CAA [22–26]. In a large single-center cohort of patients with ICH, high CSO-EPVS degree was associated with MRI markers of CAA (i.e., lobar CMB and cSS) whereas high BG-EPVS degree was associated with MRI markers of HA [11]. This link between CSO-EPVS and CAA was recently confirmed in two cohorts of patients with inherited and pathologically proven sporadic CAA [26].

Our study demonstrated the association between EPVS topography and vascular amyloid load assessed by 18F-florbetapir amyloid PET. We found that among patients with primary ICH, high CSO-EPVS degree was associated with florbetapir PET positivity whereas high BG-EPVS degree was not. Moreover, approximatively 60% of patients with a CSO-EPVS predominance pattern had a positive florbetapir PET compared with none with a BG-EPVS predominance pattern. Only one previous study including 11 patients with CAA-ICH and 20 healthy controls investigated the association between amyloid PET and EPVS, using 11C-Pittsburgh compound B (PiB), another amyloid radiotracer [27]. The burden of CSO-EPVS (but not BG-EPVS) was associated with PiB retention across the whole cohort. However, this

Table 3 Logistic regression of factors associated with CSO-EPVS high (grade > 2) degree

	Univariable analysis			Multivariable analysis[c]		
	OR	95% CI	*p* value	OR	95% CI	*p* value
Age (per each year older)	1.07	1.00–1.16	0.08	–		–
Female sex	1.25	0.32–4.83	0.75	–		–
Hypertension[a]	0.19	0.04–0.74	0.02	–		–
Diabetes[a]	0.63	0.08–3.48	0.62	–		–
Florbetapir PET positivity[a]	6.67	1.56–33.36	0.01	6.44	1.32–38.93	0.03
Strictly lobar CMB[a]	2.43	0.62–9.91	0.20	–		–
cSS[a]	2.85	0.67–12.74	0.16	–		–
Severe WMH[a,b]	6.07	1.51–28.90	0.02	5.87	1.28–33.48	0.03
ApoE ε2 and/or ε4 allele[a]	2.25	0.55–9.49	0.26	–		–

[a] Presence vs. absence

[b] Fazekas' score 5 or 6

[c] Adjusted for age, history of hypertension, strictly lobar CMB (presence), cSS (presence), severe WMH, and florbetapir PET positivity

CI, confidence interval; *CMB*, cerebral microbleeds; *CSO-EPVS*, enlarged perivascular spaces in the centrum semiovale; *cSS*, cortical superficial siderosis; *OR*, odds ratio; *WMH*, white matter hyperintensities

association was not significant when analysis was restricted to CAA patients, probably due to the limited sample size of this subgroup. Results from these two amyloid PET studies are in line with a recent post-mortem MRI study that demonstrated that CSO-EPVS degree was associated with CAA histopathological severity [28].

The strengths of this study include its prospective design, a systematic multimodal evaluation (3T research MRI and 18F-florbetapir PET) of patients with primary ICH, and the use of well-characterized EPVS patterns. Our study has also limitations. Although close to those from other amyloid PET studies in ICH cohorts [13, 29], the sample size was relatively small, and our study was likely underpowered, especially in multivariable analyses. Confidence intervals are wide, and results should be cautiously interpreted. Nonetheless, our findings linking CSO-EPVS to CAA are consistent with previous studies using other markers of CAA (MRI markers, histopathological scale, PiB PET) [11, 26–28]. Hence, our results should be considered preliminary and require external validation. In the absence of a validated threshold value of florbetapir SUVr to define positive CAA cases, florbetapir PET was visually assessed that may appear as a more subjective method. However, the raters were blind to ICH location for the visual assessment of florbetapir PET, and results of our sensitive analysis based on a threshold value of SUVr to define florbetapir positivity are consistent—though not statistically significant—with the visual analysis. Additionally, amyloid imaging cannot accurately differentiate vascular amyloid from parenchymal amyloid whereas co-occurrence of AD is common in CAA patients [30]. Although patients with preexisting cognitive impairment assessed by IQCODE were excluded from our study to minimize the risk of AD, we cannot totally rule out the presence of AD pathology in patients with CAA-related lobar ICH, as well as in patients with deep ICH. Finally, our findings may only be applicable to a selected ICH population, specifically the less severe cases able to have brain MRI and those without pre-ICH cognitive impairment.

Conclusion

Our findings provide further supporting evidence that among patients with spontaneous ICH, severe CSO-EPVS are markers of vascular amyloid burden whereas BG-EPVS are not, suggesting that the anatomical distribution of EPVS may reflect the underlying vasculopathy. Ongoing collaborative studies with pathologically proven CAA vs. non-CAA cases should assess whether CSO-EPVS would enhance diagnostic accuracy of the MRI-based Boston criteria.

Acknowledgments The authors thank the promoter of this study, CHU Toulouse.

Funding This study was funded by Avid Radiopharmaceuticals, Toulouse Teaching Hospital (CHU) (local grant 2011 to N.R.) and the Institut des Sciences et du Cerveau de Toulouse. Avid Radiopharmaceuticals provided funding for the PET scanning and supplied the florbetapir precursor. This work has been in part supported by a grant from the French National Agency for Research called "Investissements d'Avenir" No. ANR-11-LABEX-0018-01. This work was supported by CHU Toulouse for regulatory and ethical approval and compliance. Nicolas Raposo was supported by a Fulbright

Scholarship and received an Arthur Sachs Scholarship from the Harvard University Committee on General Scholarship and a Philippe Foundation research grant.

Data availability The data that support the findings of this study are available from the corresponding author on reasonable request.

Compliance with ethical standards

Conflict of interest Dr. Payoux reports personal fees from Lilly/Avid and from GE Heathcare. Dr. Albucher received consulting fees from Bayer and speaker honoraria from Boehringer Ingelheim, Bayer, and Pfizer. Dr. Calviere received consulting fees from Boehringer Ingelheim and travel grant from Boehringer Ingelheim and Pfizer. Dr. Chollet served as a consultant for Institut de Recherche Pierre Fabre and has received speaker honoraria from Bristol-Myers Squibb and Boston Scientific. Dr. Olivot received consulting fees from AstraZeneca, Servier, and Boston Scientific and speaker honoraria from Boehringer Ingelheim, Pfizer, and Bristol-Myers Squibb. Dr. Pariente is an associate editor of the Journal of Alzheimer's Disease and has received speaker honoraria from Lilly, Roche, and Novartis. All other authors declare that they have no conflict of interest.

Role of the funder The funders had no role in the design or conduct of the study; in the collection, management, analysis, or interpretation of the data; in the preparation, review, or approval of the manuscript; or in the decision to submit the manuscript for publication.

Ethical approval All procedures performed in studies involving human participants were in accordance with the ethical standards of the institutional research committee (Toulouse-Purpan Hospital Ethical Standards Committee on Human Experimentation; No. 1122302) and with the principles of the 1964 Declaration of Helsinki and its later amendments or comparable ethical standards.

Informed consent Informed consent was obtained from each participant (or a legally authorized representative) included in the study.

References

1. Qureshi AI, Tuhrim S, Broderick JP, Batjer HH, Hondo H, Hanley DF. Spontaneous intracerebral hemorrhage. N Engl J Med. 2001;344(19):1450–60.
2. Pantoni L. Cerebral small vessel disease: from pathogenesis and clinical characteristics to therapeutic challenges. Lancet Neurol. 2010;9(7):689–701.
3. Charidimou A, Gang Q, Werring DJ. Sporadic cerebral amyloid angiopathy revisited: recent insights into pathophysiology and clinical spectrum. J Neurol Neurosurg Psychiatry. 2012;83(2):124–37.
4. Wardlaw JM, Smith C, Dichgans M. Mechanisms of sporadic cerebral small vessel disease: insights from neuroimaging. Lancet Neurol. 2013;12(5):483–97.
5. Viswanathan A, Rakich SM, Engel C, Snider R, Rosand J, Greenberg SM, et al. Antiplatelet use after intracerebral hemorrhage. Neurology. 2006;66(2):206–9.
6. Biffi A, Halpin A, Towfighi A, Gilson A, Busl K, Rost N, et al. Aspirin and recurrent intracerebral hemorrhage in cerebral amyloid angiopathy. Neurology. 2010;75(8):693–8.
7. Greenberg SM, Vernooij MW, Cordonnier C, Viswanathan A, Al-Shahi Salman R, Warach S, et al. Cerebral microbleeds: a guide to detection and interpretation. Lancet Neurol. 2009;8(2):165–74.
8. Linn J, Halpin A, Demaerel P, Ruhland J, Giese AD, Dichgans M, et al. Prevalence of superficial siderosis in patients with cerebral amyloid angiopathy. Neurology. 2010;74(17):1346–50.
9. Wardlaw JM, Smith EE, Biessels GJ, Cordonnier C, Fazekas F, Frayne R, et al. Neuroimaging standards for research into small vessel disease and its contribution to ageing and neurodegeneration. Lancet Neurol. 2013;12(8):822–38.
10. Weller RO, Hawkes CA, Kalaria RN, Werring DJ, Carare RO. White matter changes in dementia: role of impaired drainage of interstitial fluid. Brain Pathol. 2015;25(1):63–78.
11. Charidimou A, Boulouis G, Pasi M, Auriel E, van Etten ES, Haley K, et al. MRI-visible perivascular spaces in cerebral amyloid angiopathy and hypertensive arteriopathy. Neurology. 2017;88(12):1157–64.
12. Hawkes CA, Jayakody N, Johnston DA, Bechmann I, Carare RO. Failure of perivascular drainage of beta-amyloid in cerebral amyloid angiopathy. Brain Pathol. 2014;24(4):396–403.
13. Gurol ME, Becker JA, Fotiadis P, Riley G, Schwab K, Johnson KA, et al. Florbetapir-PET to diagnose cerebral amyloid angiopathy: a prospective study. Neurology. 2016;87(19):2043–9.
14. Raposo N, Planton M, Peran P, Payoux P, Bonneville F, Lyoubi A, et al. Florbetapir imaging in cerebral amyloid angiopathy-related hemorrhages. Neurology. 2017;89(7):697–704.
15. Jorm AF. The Informant Questionnaire on Cognitive Decline in the Elderly (IQCODE): a review. Int Psychogeriatr. 2004;16(3):275–93.
16. Charidimou A, Linn J, Vernooij MW, Opherk C, Akoudad S, Baron JC, et al. Cortical superficial siderosis: detection and clinical significance in cerebral amyloid angiopathy and related conditions. Brain. 2015;138(Pt 8):2126–39.
17. Fazekas F, Chawluk JB, Alavi A, Hurtig HI, Zimmerman RA. MR signal abnormalities at 1.5 T in Alzheimer's dementia and normal aging. AJR Am J Roentgenol. 1987;149(2):351–6.
18. Doubal FN, MacLullich AM, Ferguson KJ, Dennis MS, Wardlaw JM. Enlarged perivascular spaces on MRI are a feature of cerebral small vessel disease. Stroke. 2010;41(3):450–4.
19. Maclullich AM, Wardlaw JM, Ferguson KJ, Starr JM, Seckl JR, Deary IJ. Enlarged perivascular spaces are associated with cognitive function in healthy elderly men. J Neurol Neurosurg Psychiatry. 2004;75(11):1519–23.
20. Johnson KA, Sperling RA, Gidicsin CM, Carmasin JS, Maye JE, Coleman RE, et al. Florbetapir (F18-AV-45) PET to assess amyloid burden in Alzheimer's disease dementia, mild cognitive impairment, and normal aging. Alzheimers Dement. 2013;9(5 Suppl):S72–83.
21. Zhu YC, Tzourio C, Soumare A, Mazoyer B, Dufouil C, Chabriat H. Severity of dilated Virchow-Robin spaces is associated with age, blood pressure, and MRI markers of small vessel disease: a population-based study. Stroke. 2010;41(11):2483–90.
22. Banerjee G, Kim HJ, Fox Z, Jager HR, Wilson D, Charidimou A, et al. MRI-visible perivascular space location is associated with Alzheimer's disease independently of amyloid burden. Brain. 2017;140(4):1107–16.
23. Martinez-Ramirez S, Pontes-Neto OM, Dumas AP, Auriel E, Halpin A, Quimby M, et al. Topography of dilated perivascular spaces in subjects from a memory clinic cohort. Neurology. 2013;80(17):1551–6.
24. Charidimou A, Meegahage R, Fox Z, Peeters A, Vandermeeren Y, Laloux P, et al. Enlarged perivascular spaces as a marker of underlying arteriopathy in intracerebral haemorrhage: a multicentre MRI cohort study. J Neurol Neurosurg Psychiatry. 2013;84(6):624–9.
25. Charidimou A, Jaunmuktane Z, Baron JC, Burnell M, Varlet P, Peeters A, et al. White matter perivascular spaces: an MRI marker in pathology-proven cerebral amyloid angiopathy? Neurology. 2014;82(1):57–62.

26. Charidimou A, Hong YT, Jager HR, Fox Z, Aigbirhio FI, Fryer TD, et al. White matter perivascular spaces on magnetic resonance imaging: marker of cerebrovascular amyloid burden? Stroke. 2015;46(6):1707–9.
27. Martinez-Ramirez S, van Rooden S, Charidimou A, van Opstal AM, Wermer M, Gurol ME, et al. Perivascular spaces volume in sporadic and hereditary (Dutch-type) cerebral amyloid angiopathy. Stroke. 2018;49(8):1913–9.
28. van Veluw SJ, Biessels GJ, Bouvy WH, Spliet WG, Zwanenburg JJ, Luijten PR, et al. Cerebral amyloid angiopathy severity is linked to dilation of juxtacortical perivascular spaces. J Cereb Blood Flow Metab. 2016;36(3):576–80.
29. Ly JV, Donnan GA, Villemagne VL, Zavala JA, Ma H, O'Keefe G, et al. 11C-PIB binding is increased in patients with cerebral amyloid angiopathy-related hemorrhage. Neurology. 2010;74(6):487–93.
30. Boyle PA, Yu L, Nag S, Leurgans S, Wilson RS, Bennett DA, et al. Cerebral amyloid angiopathy and cognitive outcomes in community-based older persons. Neurology. 2015;85(22):1930–6.